OPTIMIZATION OF REFUELING SCHEDULE FOR LIGHT-WATER REACTORS

FUEL CYCLES

KEYWORDS: *PWR-type reactors, BWR-type reactors, optimization, fuel management*

HIROSHI MOTODA,* JOHN HERCZEG,** and ALEXANDER SESONSKE *Purdue University*
Department of Nuclear Engineering
West Lafayette, Indiana 47907

Received April 3, 1974
Accepted for Publication August 26, 1974

A stagewise optimization of the refueling schedule for light-water reactors has been developed with emphasis on the nuclear model. The decision variables to be determined are end-of-cycle (EOC) reactivity distribution, energy output, power distribution, number of fresh fuel assemblies, number of reinsertion of used assemblies, selection of assemblies for discharge, and allocation of each fuel assembly in a two-dimensional core geometry.

Division of the total problem into six phases permits usage of the most effective method in each phase. This study employed such techniques as linear programming for regionwise shuffling optimization, linear iterative search for the optimal EOC state, the minimum integrated k-deviation method for a guess allocation, and direct search for the optimal allocation of each fuel assembly, etc., all of which are interrelated.

The applicability of this method to a commercial light-water reactor was demonstrated for a 1300-MW(th) boiling-water reactor by successfully generating a ten-cycle refueling schedule using a fixed enrichment of initial and reload fuel and allowing reinsertion of discharged fuel assemblies from the first to the third cycles.

The results indicate a savings of as much as 14% of the fresh fuel consumption over a conventional mixed four- and five-batch scatter loading, with thermal characteristics well within design limits.

I. INTRODUCTION

The nuclear-fuel-cycle cost for a light-water reactor (LWR) is strongly influenced by the in-core fuel management scheme. Treatment of the nuclear core loading as an optimization problem over the entire reactor life can reduce fuel consumption by a minimum of 10%. For a typical large boiling-water reactor (BWR), this would mean an annual savings in the cost of nuclear fuel of ~$350 000 (Ref. 1). In addition, the large demand for light-water nuclear fuel in the early 1980's further suggests the need for optimization of the in-core nuclear fuel management.

Due to the size of the problem, complete optimization of a refueling scheme for the entire reactor lifetime is a tremendous task. The primary reason for this is the large number of decision variables and the complexity of the system. Several investigators have tried to simplify the approach by formulating a mathematical problem that could be successfully solved by various optimization techniques, such as dynamic programming,[2,3] variational methods,[4,5] and heuristic methods.[6,7] When the number of variables became too large to handle by a simple formulation, a new approach was suggested which separated the total problem into coupled subproblems, each of which utilizes the best optimization techniques. Mélice[8] was the first to propose this approach and separated the problem into two subproblems: (a) determination of the number and enrichments of fresh fuel assemblies, and (b) determination of the initial boron concentration and the refueling pattern in which the fresh fuel and recovered assemblies are to be loaded. Using an optimal k profile complying with the maximum power (minimum peaking factor) condition and cycling diagram, Mélice applied this method to an analysis of the stationary and transi-

*Present address: Atomic Energy Research Laboratory, Hitachi, Ltd., Ozenji, Kawasaki, Kanagawa Pref. 215, Japan.
**Present address: Brookhaven National Laboratory, Upton, Long Island, New York 11973.

ent cycles of the SENA pressurized-water reactor (PWR) with a three-region mixed mode.

Thomsen[9] employed a similar approach to a one-dimensional core model of a BHWR and the Yankee (PWR) reactor. In his approaches, several automated shuffling methods were presented by assuming a fixed enrichment and batch fraction for new assemblies.

Sauer[10] separated internal decisions (those which affect the operation of the reactor) from external decisions (those which interrelate with overall fuel management or total energy production). Sauar's approach provides a systematic procedure for an internal fuel-cycle optimization problem employing linear programming to optimize fuel shuffling for a few-region BWR.

Suzuki and Kiyose[11] applied linear programming to determine internal decision variables in terms of Sauar's definition. Suzuki and Kiyose calculated a refueling schedule of a five-region-core BWR over ten cycles without detailing the optimal allocation of each fuel assembly to a two-dimensional array.

Naft and Sesonske[12] developed a direct search algorithm to optimize the fuel shuffling pattern and applied it to the San Onofre PWR. In their application, only part of the internal decision variables were considered.

Howland et al.[13] separated the fuel shuffling problem into two stages: (a) the finding of an optimal k profile by the gradient projection methods, and (b) the allocation of each assembly to best fit the reference k profile by the Monte Carlo method. Howland's approach also considered only a part of the internal decision variables.

In another approach, Chitakara and Weisman[14] related the movement of each fuel assembly to fuel-cycle cost by assuming an equilibrium cycle and applying a standard assignment problem technique.

The approaches discussed above indicate the necessity of developing a method to optimize both the internal and external problems, with greatest stress on the nuclear model in a reasonable amount of computer time.

In an attempt to satisfy the above requirements, a computer program (OPREF) was developed which generates an optimal refueling schedule in a two-dimensional nuclear-thermal-hydraulic-coupled model. This method builds on the contributions of many previous investigators, particularly Thomsen,[9] Sauar,[10] Suzuki and Kiyose,[11] and Naft and Sesonske.[12]

II. GENERAL INFORMATION

The formulation of the problem is based on two assumptions which permit decomposition of the total problem into several phases:

1. The burnup characteristics of each assembly can be calculated separately.
2. The state of the reactor core can be represented by a k_∞ distribution.

The first assumption permits use of the FLARE-type fitting formulation[15] applied to burnup calculations without solving the burnup chain equation. The second assumption implies that there is a one-to-one correspondence between the k_∞ and k_{eff} distribution. Thus, the power distribution and k_{eff} can be approximately calculated without knowing the actual fuel distribution.

A refueling schedule can generally be expressed as a multistage decision process. The cost of cycle j can be expressed as

$$Z_j = f(\mathrm{X}_{j-1}, W_j) \quad , \tag{1}$$

where X_j defines the end-of-cycle (EOC) state of cycle j and W_j defines the decision vector at cycle j. Thus, the minimization of the total cost, J_0, over the entire life is

$$\min J_0 = \min_{\{W_j\}} \sum_{j=1}^{J} f(\mathrm{X}_{j-1}, W_j) \quad . \tag{2}$$

The components of the decision vector, W_j, which are to be determined at each cycle j are as follows:

1. operating period	Δt_j
2. EOC reactivity distribution	$k_{\infty j}^{\text{EOC}}(r)$
3. energy output	$E_{n_j}(r)$
4. power distribution	$P_j(r, t)$
5. control-rod distribution	$C_j(r, t)$
6. enrichment of fresh fuel	ϵ_j
7. number of fresh assemblies	G_j
8. number of reinsertion of used assemblies	G_j
9. selection of assemblies for discharge	G_j
10. shuffling scheme.	

The following constraints must be taken into consideration:

1. burnup limit
2. residence time limit
3. power density limit
4. heat flux limit
5. local reactivity limit (stuck-rod margin).

The decision vector W_j can be divided into two subvectors based on the second assumption above:

$$W_j = (W_{j0}, G_j) \quad , \tag{3}$$

where

$$W_{j0} = [\Delta t_j, k_{\infty j}^{EOC}(r), E_{n_j}(r), P_j(r,t), C_j(r,t), \epsilon_j]$$

G_j = description of the refueling scheme.

The beginning-of-cycle (BOC) state, $k_{\infty j}^{BOC}(r)$, can be calculated by assuming $k_{\infty j}^{EOC}$ and $E_{n_j}(r)$ [assumption (1)]. The power distribution, $P_j(r, t)$, is determined by $C_j(r, t)$. If a $C_j(r, t)$ exists that can transfer the state from $k_{\infty j}^{BOC}(r)$ to $k_{\infty j}^{EOC}(r)$ without violating constraints (4) and (5), the trajectory itself has no influence on the cost. In other words, the optimization of control-rod programming should be considered only in determining the optimal terminal state, $k_{\infty j}^{EOC}(r)$, and the optimal energy output, $E_{n_j}(r)$, and is separable from the determination of G_j. A discussion of optimal terminal state (OTS) is given in Ref. 16. Thus, W_{j0} can be written as

$$W_{j0} = W_{j0}' = [\Delta t_j, k_{\infty j}^{EOC}(r), E_{n_j}(r), \epsilon_j] \quad . \tag{4}$$

The vector, G_j, can be regarded as the variables of the internal optimization problem which should be solved using W_{j0}' as the boundary condition:

$$G_j = G_j(W_{j0}') \quad . \tag{5}$$

Under this condition, Eq. (2) can be separated into a two-stage optimization problem:

$$J_0 = \min_{\{W_{j0}'\}} \left[\min_{\{G_j\}} \sum_{j=1}^{J} f(x_{j-1}, W_j) \right] \quad . \tag{6}$$

Of the components of W_{j0}, ϵ_j is most affected by constraint 2 and is separated from the other constraints as follows:

$$W_{j0}' = (W_{j0}'', \epsilon_j) \quad .$$

The decision vector, G_j, describes the refueling scheme. For convenience, G_j is separated into two parts:

1. regionwise shuffling—the decisions, G_{j0}, as to the kind of assemblies that should be in each region
2. the optimal allocation of each fuel assembly in each region in a two-dimensional geometry.

Thus,

$$G_j = (G_{j0}, \text{allocation of fuel assemblies}) \quad . \tag{8}$$

The cost, J_0, [Eq. (6)] is assumed to depend only on G_{j0}; therefore, the optimal allocation can be performed on the basis of a minimum mismatch factor. A five-region core model is sufficient for implementing this problem. A flow diagram of the general procedure discussed above is shown in Fig. 1.

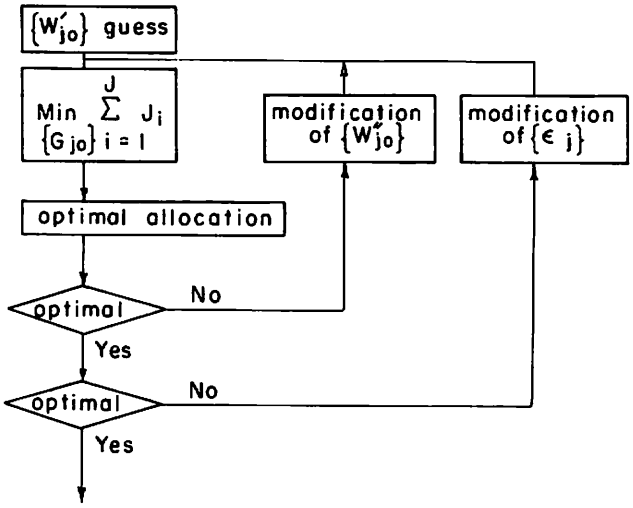

Fig. 1. General optimization procedure of the refueling schedule.

III. STAGEWISE OPTIMIZATION

Linear programming can be applied to determine $\{G_j\}$ for a given set of $\{W_{j0}\}$. For this application, the methods of Sauar[10] and Suzuki and Kiyose[11] are briefly reviewed. Sauar defined the term "lot" as a group of assemblies that have the same history. Numeration of the different histories permits classification of assemblies into a number of different lots, I. The number of assemblies in each lot can be determined by a linear programming code. Application of linear programming takes into account regionwise reactivity and material balance, and minimizes the fuel-cycle cost.

Sauar's approach,[10] when applied to a five-region nuclear core model, produces as many as 6×10^8 lots. Application of the residence time limit (e.g., 5 yr) constraint reduces the number of lots to $\sim 8 \times 10^4$, which still yields the number of variables of 80 000 and the number of constraints of 100. Assuming the equilibrium loading from the sixth cycle on and limiting I to 116, Sauar applied this method to a two-region ten-cycle model of a BWR. Thus, the problem contained only 116 variables and 40 constraints and could be easily solved. Direct application of this method to a more realistic five-region model appears to be impractical.

Suzuki and Kiyose[11] defined the fuel loading matrices α_{ki}^j and β_{ki}^j, which describe how many fuel assemblies of burnup level, i, are loaded into region k at cycle j, as the method to express the fuel loading state at each cycle (where α and β refer to the BOC and EOC, respectively). Once W_{j0} is given, the burnup level, i, of each region, k,

can be precalculated by considering all the possible histories of fuel assemblies. The corresponding $k_{\infty ki}^{EOC^j}$ and the transfer relation from α to β can also be calculated. Suzuki and Kiyose also used linear programming to minimize the fresh fuel assemblies requirement for a five-region model of a BWR by applying a regionwise mass, reactivity, and energy balance, as well as a continuity constraint. This problem was carried through ten cycles under a no-reinsertion model by assuming a flat $k_{\infty k}^{BOC}$ and a Haling power distribution,[17] which is independent of cycle j. The number of variables and constraints was 8208 and 1890, respectively. Computation time was ~5 h using a CDC 3600 computer. With regard to the optimization of W_{j0}, this approach also seems impractical. However, an interesting result was obtained by solving the J stagewise optimization problems, which provide an initial feasible solution to the original problem. The results indicated that the total number of fresh fuel assemblies necessary was only 0.7% larger than the result of overall optimization; furthermore, the stagewise optimization gave the simpler shuffling scheme. In addition, the number of fresh fuel assemblies loaded in each region approached an equilibrium. This stagewise problem can be solved in several minutes.

Investigation of these previous approaches led us to conclude that an overall optimization of a five-region core model cannot be performed on today's computers within a reasonable time. A stagewise optimization approach is therefore suggested as a means of solution.

Optimum use of fresh fuel assemblies is of direct interest to a utility primarily because refueling intervals are usually prescribed and the capacity factor within a given time interval may vary depending on dispatching parameters. It is generally desirable to have the capacity factor as high as possible. Therefore, a performance index can be the number of fresh fuel assemblies loaded in each cycle instead of fuel-cycle cost calculated in a simplified manner.

In Fig. 1, where the overall optimization approach is shown, the improvement of $\{W_{j0}\}$ is performed after the decision of $\{G_{j0}\}$. However, in the stagewise optimization, a straightforward solution is obtained by iterating on G_{j0} and W_{j0} in each cycle.

IV. NUCLEAR MODEL

One of the main objectives of this work was to develop a method to optimize the allocation of each fuel assembly in a BWR. It would be desirable to employ a three-dimensional nuclear-thermal-hydraulic-coupled model to calculate the power distribution throughout the reactor. However, the computer time necessary for such a model would be on the order of several hours. As a compromise method, a two-dimensional FLARE-type nodal equation was developed. The thermal-hydraulic treatment is similar to that employed by FLARE. Improvement was made on the fitting formula of the infinite multiplication factor as a function of burnup, burnup-weighted void, power, void, and control fraction. The transport kernel was divided by k_∞ of its node.[18] Input data to this program, named MODFLA, are essentially the same as FLARE with the exception that a standard axial power distribution must be provided to calculate the axially averaged void distribution. Computer running time for MODFLA is ~4 sec on a CDC 6500 for a normal power distribution calculation, and 40 sec for a Haling power distribution calculation which makes the reactor critical.

The accuracy of this method was compared with a three-dimensional FLARE calculation. The results, using different control-rod patterns, indicated an error in the eigenvalue, λ, channelwise power, P_{ij}, moderator density, U_{ij}, and infinite multiplication factor, k_{ij}, of 0.05, 5.0, 5.0, and 0.5%, respectively. These errors are considered within acceptable limits.

Other parameters, such as maximum fractional linear power density (MFLPD) and minimum critical heat flux ratio (MCHFR) are estimated by

$$\text{MFLPD} = \max_{ij} \text{FLPD}_{ij} \times P_{kax}$$

$$\text{MCHFR} = \min_{ij} \text{CHFR}_{ij} / P_{kax} \quad ,$$

where P_{kax} is the axial power peaking factor. The refueling and shuffling simulation is performed by designating the assembly labels in a two-dimensional array.

V. OPTIMIZATION PROCEDURE

The basic approach described in Secs. II and III is divided into six phases, as is shown in Fig. 2. To save computer time, the optimization of G_{j0} is separated into two parts: a three-region and a five-region core model. A linear programming code was coupled with MODFLA for the purpose of iterating in W'_{j0} and G_{j0} for a three-region model. The search for W_{j0} is essentially one-dimensional due to the employment of the minimum fuel inventory principle. The optimal three-region W'_{j0} is extended to a five-region W'_{j0}, and a more accurate linear program is employed to solve for a final G_{j0}.

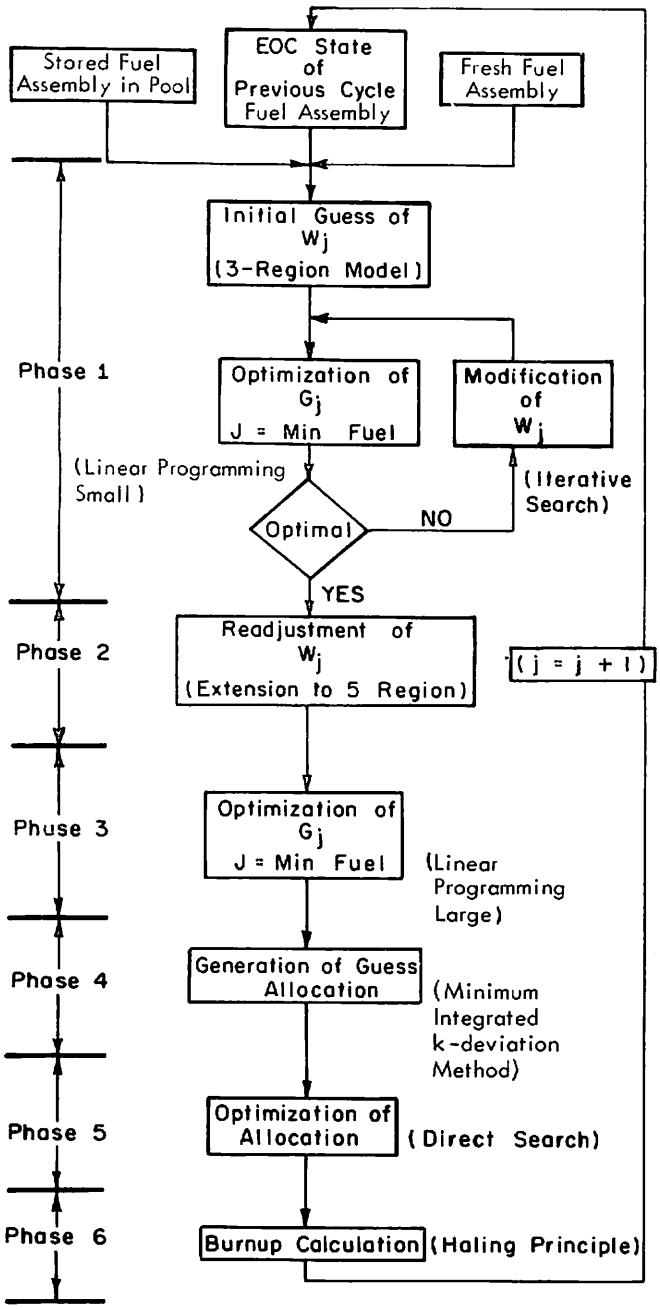

Fig. 2. Calculational flow diagram of stagewise optimization of the refueling schedule.

The optimal allocation problem is also divided into two parts. First, an acceptable initial guess load pattern is generated by using the minimum integrated k-deviation method. This method does not require a power distribution calculation and thus significantly reduces the optimization time. By employing the obtained guess allocation, a more time-consuming direct search method is applied to optimize the assembly allocation such that the power peaking factor is minimized.

The optimization procedure is performed at the estimated EOC state where all the control rods are withdrawn. The power distribution can be controlled by control-rod movement as well as by fuel shuffling at BOC. To optimize both at the same time is rather a complex problem and is contrary to the basic assumption that the effect of control-rod programming is separated from fuel management through the optimal terminal state.

Previous studies[16,19] have indicated that although optimal control-rod programming differs from that employing the Haling power distribution, at any instant the optimal EOC state W'_{j0} does not differ significantly from that of a Haling distribution for current design criteria on power peaking. On this basis, the Haling power distribution was assumed to transfer the reactor from BOC to EOC.

As a last step, a burnup calculation is performed for the optimized assembly allocation. The Haling power distribution and cycle length are reevaluated; then the next cycle procedure is repeated. A more detailed description is given below.

V.A. Phase 1

The first part of phase 1 is a file system in which the histories of all the fuel assemblies are stored. This file is composed of the following.

1. state of the fuel assemblies at EOC of the previous cycle
2. stored fuel assemblies in the pool which have been used in previous cycles
3. fresh fuel assemblies.

The discharged fuel assemblies are newly added to this file at the end of each cycle. Burnup, E, burnup-weighted void, V, and residence time, RT, of the fuel assemblies in the core are renewed at the end of each cycle in the program MODFLA. This file is the input to phase 1.

The problem is to determine the components of decision vectors W'_{j0} and G_{j0} for a three-region core model. The approach is as follows:

V.A.1. Optimization of G_{j0}

The result should be expressed in terms of the number of fuel assemblies of each type. This type of problem requires integer linear programming which has the capacity to handle hundreds of variables and constraints. Since such a program is not readily available, two linear programming methods are applicable. One method is to use 0, 1

programming, in which the fresh fuel assemblies have to be distinguished from each other by artificially changing the nuclear properties slightly; thus, each variable should be reduced to have a value of either 0 or 1. Another method is to use standard linear programming. In this case, fuel burnup is levelized to include several assemblies in each level, and all the assemblies in each level are assumed to have the same nuclear property. Levelization facilitates integerization of the results and reduces the scale of the problem. The application of standard linear programming is therefore possible. Here, the standard programming method is applied.

At this stage, the residence time limit constraint can be checked. The computer program checks assembly n to determine if the cycle length plus the residence time exceeds the maximum residency time. The remaining assemblies are rearranged in order of increasing burnup for each fuel type.

After assigning the fresh fuel assemblies to level 1, new fuel assemblies, named the "collapsed fuel assembly file," are generated by levelizing the assemblies with level width of ΔB in GWd/T (gigawatt-days/tonne). Burnup, burnup-weighted void, and residence time are averaged over the assemblies in the same level with the fuel assembly labels undefined.

Among the other constraints, the average burnup limit is related to the enrichment of the fresh fuel assemblies and can be treated separately. Power density, heat flux, and local reactivity can also be taken into account in a global form for the optimization of the components of W_{j0}'. The optimal allocation of fuel assemblies in a two-dimensional array in phases 4 and 5 is aimed at minimizing the power peaking, thus indirectly satisfying the above constraints. Derating condition can be included in W_{j0}'. Thus, only the maximum burnup limit and local reactivity constraint need be considered at this stage of the determination of G_{j0}.

The burnup increment, $\Delta E_{l,k}$, of the fuel assemblies at level l in region k can be expressed as follows:

$$\Delta E_{l,k} = P_k^* \cdot f_{l,k} \cdot \Delta E \quad , \tag{11}$$

where P_k^* is the regionwise target power density and ΔE is the core-averaged burnup increment of one cycle, both of which are components of W'_{j0}. The term $f_{l,k}$ is the power mismatch factor between the adjacent assemblies.

The expression for $f_{l,k}$ is based on the assumption that the infinite multiplication factor, k_∞, and the material buckling, B^2, are the major controlling factors:

$$f_{l,k} = C_1 \frac{k'_{\infty l,k}}{k^*_{\infty k}} + C_2 \frac{B^2_{l,k}}{B^{2*}_k} \tag{12}$$

$$k'_{\infty l,k} = F(P_k^* f_{l,k}, E'_{l,k}, V'_{l,k}, U_k^*, I_{\text{type}}) \tag{13}$$

$$E'_{l,k} = E_l + \Delta E_{l,k} \tag{14}$$

$$V'_{l,k} = V_l + \Delta E_{l,k} U_k^* \tag{15}$$

$$B^2_{l,k} = (k'_{\infty l,k} - 1)/M_k^2 \quad , \tag{16}$$

where C_1 and C_2 are constants such that $C_1 + C_2 = 1.0$ and where $k^*_{\infty k}$, U_k^*, and B_k^{2*} are the target infinite multiplication factor, moderator density, and material buckling, respectively. The quantities $k'_{\infty l,k}$, $E'_{l,k}$, and $V'_{l,k}$ are the estimated EOC infinite multiplication factor, burnup, and burnup-weighted void, respectively.

Since Eq. (12) contains $k'_{\infty l,k}$, which requires knowledge of $f_{l,k}$ by Eq. (13), and since the function F is rather complicated, an iteration process is used to calculate $f_{l,k}$. The following relation must be satisfied for each region k:

$$E'_{l,k} \leq E_{\max} \quad , \tag{17}$$

where $E_{\max}$ is the maximum allowable burnup.

The constraint on local reactivity is primarily for the stuck-rod margin. Since this constraint is applied to a cold state, several difficulties arise in implementing this constraint. However, since rod worth is strongly affected by the local reactivity distribution of the surrounding assemblies, this constraint can be approximated by

$$f_{l,k} \leq f_{\text{lim}} \quad , \tag{18}$$

where f_{lim} is the maximum allowable power mismatch factor. These two constraints are checked before the linear programming calculation. By letting the number of assemblies of level l in region k be denoted as $\chi_{l,k}$, G_{j0} is then expressed

$$G_{j0} = \{\chi_{l,k}\} \quad . \tag{19}$$

It is understood in the following expression that level l in region k which violates Eqs. (17) and (18) is skipped in the operation.

The constraints for linear programming are as follows:

1. Continuity condition. The number of partially burnt fuel assemblies of each level, l, in the solution must be less than or equal to the number of assemblies in the input assembly file, which is denoted as N_{cl}:

$$\sum_{k=1}^{N_{\text{reg}}} \chi_{l,k} \leq N_{cl} \qquad l = 2, 3, \ldots, N_l \quad , \tag{20}$$

where N_{reg} is the number of regions and N_l is the maximum number of levels over all regions.

2. Mass balance. The number of fuel assemblies in each region k must be a specific number, N_{ak}:

$$\sum_{l=1}^{N_l} \chi_{l,k} = N_{ak} \qquad k = 1, 2, \ldots, N_{\text{reg}} \quad . \tag{21}$$

3. Energy balance. The average burnup increment of all fuel assemblies in each region must be equal to the target burnup increment, ΔE_k^*

By Eq. (11), the following energy balance equation is required:

$$\sum_{l=1}^{N_l} \Delta E_{l,k} \cdot \chi_{l,k} = \Delta E_k^* \cdot N_{ak}$$

$$k = 1, 2, \ldots, N_{\text{reg}} \quad . \tag{22}$$

Noting that $\Delta E_k^* = P_k^* \Delta E$, Eq. (22) can be rewritten in a simpler form:

$$\sum_{l=1}^{N_l} f_{l,k} \chi_{l,k} = N_{ak} \qquad k = 1, 2, \ldots, N_{\text{reg}} \quad . \tag{23}$$

Equation (23) states that the region-averaged power mismatch factor should be equal to 1.0.

4. Reactivity constraint. The average infinite multiplication factor of all assemblies in each region must be equal to the target infinite multiplication factor, $k_{\infty k}^*$, at EOC:

$$\sum_{l=1}^{N_l} k'_{\infty l,k} \cdot f_{l,k} \cdot \chi_{l,k} \Big/ \sum_{l=1}^{N_l} f_{l,k} \cdot \chi_{l,k} = k_{\infty k}^*$$

$$k = 1, 2, \ldots, N_{\text{reg}} \quad . \tag{24}$$

The weighting factor, $f_{l,k} \cdot \chi_{l,k}$, which is proportional to the allocated power in fuel assemblies of level l in region k, is used in place of the importance function. By employing Eq. (23) in Eq. (24), a simplified form of Eq. (24) is obtained:

$$\sum_{l=1}^{N_l} k'_{\infty l,k} \cdot f_{l,k} \cdot \chi_{l,k} = k_{\infty k}^* \cdot N_{ak}$$

$$k = 1, 2, \ldots, N_{\text{reg}} \quad . \tag{25}$$

The objective function of this problem is the number of fresh fuel assemblies:

$$J = \sum_{k=1}^{N_{\text{reg}}} \chi_{1,k} \quad . \tag{26}$$

The number of variables and constraints are $N_{\text{reg}} \cdot N_l$ and $N_l - 1 + 3 \cdot N_{\text{reg}}$, which will be 150 and 44, respectively, for a five-region 30-level problem. To investigate the nature of the problem, let a new variable, X_l, be defined by

$$X_l = \sum_{k=1}^{N_{\text{reg}}} \chi_{l,k} \quad . \tag{27}$$

Then, Eqs. (20) through (26) can be written as follows:

$$X_l \le N_{cl} \tag{28}$$

$$\sum_l X_l = \sum_k N_{ak} \equiv N_a \tag{29}$$

$$\sum_l \bar{f}_l X_l = N_a \tag{30}$$

$$\sum_l \overline{kf}_l X_l = \sum_k k_{\infty k}^* \cdot N_{ak} \equiv \bar{k}_\infty \cdot N_a \tag{31}$$

$$J = X_1 \rightarrow \min \quad , \tag{32}$$

where $\bar{f}_l$ and $\overline{kf}_l$ are defined as

$$\bar{f}_l = \frac{\sum_k f_{l,k} \cdot \chi_{l,k}}{X_l} \tag{33}$$

$$\overline{kf}_l = \frac{\sum_k k'_{\infty l,k} \cdot f_{l,k} \cdot \chi_{l,k}}{X_l} \quad . \tag{34}$$

Since Eqs. (33) and (34) include the solution $\chi_{l,k}$, which has not yet been solved, they are considered unknown constants. However, the following condition applies independently of the value of $\chi_{l,k}$:

$$\bar{f}_l > \bar{f}_{l+1} \quad \text{and} \quad \overline{kf}_l > \overline{kf}_{l+1} \quad . \tag{35}$$

From Eqs. (29) through (31), the following equation can be obtained:

$$\sum_l (1 + \bar{f}_l + \overline{kf}_l) X_l = (\bar{k}_\infty + 2) N_a \quad . \tag{36}$$

Then, Eq. (32) becomes

$$J = \frac{(\bar{k}_\infty + 2) N_a}{1 + \bar{f}_1 + \overline{kf}_1} - \sum_{l=2}^{N_l} \frac{(1 + \bar{f}_l + \overline{kf}_l)}{(1 + \bar{f}_1 + \overline{kf}_1)} X_l \quad . \tag{37}$$

Let

$$C_l = \frac{1 + \bar{f}_l + \overline{kf}_l}{1 + \bar{f}_1 + \overline{kf}_1} \quad .$$

Then, from Eq. (35),

$$C_2 > C_3 > \ldots > C_{N_l} \quad , \tag{38}$$

assuming one fuel type.

Thus, the optimal solution is such that χ_l should be maximized from the smaller l ($l = 2, 3, \ldots$). In other words, it is desirable to discharge fuel assemblies from those which have the largest burnup. This suggests the existence of a threshold level.

The next problem is how to determine X_l. This question is very important because if it is possible to calculate X_l without solving $\chi_{l,k}$, it may be possible to optimize other functionals. In the above formulation, however, it is not possible to solve X_l in advance because the solution of X_l depends on the unknown coefficients $\bar{f}_l$ and $\overline{kf}_l$, which are determined only after the solution $\chi_{l,k}$ has been obtained. Thus, $\chi_{l,k}$ as well as X_l must be determined by solving Eqs. (20) through (26).

V.A.2. Optimization of W'_{j0}

The problem at this stage is to determine the optimal W'_{j0} that yields the minimum number of fresh fuel assemblies. Since k_∞^{EOC} determines the power distribution and if k_∞^{EOC} permits criticality at EOC, with all control rods removed, then the k_∞ distribution at BOC can be obtained by a time reversal integration of the power distribution at EOC. This method is based on the assumption that the k_∞ distribution at BOC may not be flat within each region. On the other hand, if we assume that the k_∞ distribution at BOC would be flat in each region, then the k_∞ distribution at EOC is also not flat. Such an approach requires calculating the Haling power distribution. The first method gives a smaller fuel inventory at BOC due to the more desirable k_∞ distribution. What should be determined here is a region-averaged $k^*_{\infty k}$, not a detailed k_∞ distribution across the core. On this basis, the first method was chosen from the computational standpoint.

The optimal loading principle states that the fuel assemblies with better nuclear properties should be placed toward the center of the core so long as the power-peaking constraint is not violated.[16,20] The search for W'_{j0} is essentially one-dimensional for the three-region core model. The value of k_∞ for the first region can be determined by the power-flattening principle, leaving only one degree of freedom for k_∞ in the second and third regions due to the criticality condition.

Other constraints that must be taken into account are the power density limit and the local reactivity limit in a global manner:

$$\max P_{ij} \le P_{\max} \qquad (39)$$

$$|k_{\infty k}^{EOC} - k_{\infty k+1}^{EOC}| \le \Delta k_{\max} \qquad k = 1, 2 \quad . \qquad (40)$$

Since the characteristics of fuel assemblies that are placed into this phase differ from cycle to cycle, the optimal W'_{j0} and G_{j0} also differ from cycle to cycle. In other words, $k^*_{\infty 2}$ and $k^*_{\infty 3}$ depend on the history of fuel assemblies. Criticality is attained by adjusting the region-averaged burnup of the second region, E_2, for each value of the region-averaged burnup of the third region, E_3, which is a parameter to be optimized. The criticality search is based on successive quadratic interpolation using the three latest pieces of data in a two-dimensional geometry (MODFLA).

Physical insight indicates that the optimal W_{j0} is the one that produces the smallest fissile material inventory (smallest $\int k_\infty dv$) among those in which there exists a feasible solution to the linear programming calculation. In other words, the problem is reduced to determining the largest E_3 under the constraints indicated by Eqs. (39) and (40), beyond which there is no feasible solution, G_{j0}, for linear programming problem.

V.B. Phase 2

In phase 2, an extrapolation of the optimal W'_{j0} of phase 1 is made to accommodate a five-region core model, each region containing nearly the same number of assemblies. A guess distribution of W'_{j0} is prepared by remodeling the three-region result again with the knowledge of the optimal k_∞ distribution for a minimum fuel inventory problem.[20] Since this guess distribution may not satisfy the criticality condition, an accurate criticality is achieved by readjusting the burnup level of E_3 and E_4 by employing MODFLA. After several trials, the preparation of a guess distribution has been automated. The following constraints, equivalent to Eq. (40), are imposed:

$$|k_{\infty k}^{EOC} - k_{\infty k+1}^{EOC}| \le \Delta k_{\max_2} \qquad k = 1, 2, \ldots, 4 \quad . \qquad (41)$$

V.C. Phase 3

By using the extrapolated W'_{j0}, an optimization is again performed for G_{j0} for a five-region core model. After the solution is obtained, the results $\{\chi_{l,k}\}$ are integerized in the following manner:

1. Round off to the next larger integer if the first digit after the decimal point is greater than or equal to five and vice versa.

2. Determine the threshold level, N_{thres}.

3. Check the continuity condition for levels, $1 \le l \le N_{\text{thres}}$.

4. Modify the results if item 3 is not satisfied.

5. Check the mass balance in each region; if unsatisfied, redistribute the fuel assemblies among regions in the lowest possible level.

Although round-off operation may produce consistent integerized results for most cases, provision is made to cope with an inconsistent result. At this stage, regionwise movement of all assemblies has been specified. The problem is to determine their optimal allocation in a two-dimensional grid.

V.D. Phase 4

The resultant G_{j0} of phase 3 satisfies the target distribution, W'_{j0}, and constraints 3, 4, and 5 in a region-averaged application. The allocation of assemblies is performed on the basis of a minimum power mismatch among the nearby assemblies. Phase 4 provides a good initial guess allocation without solving a two-dimensional power distribution. The method employed here is

the minimum integrated k-deviation method (MIKDM), an extension of Thomson's minimum integrated Q-deviation method[9] to a two-dimensional geometry.

The problem is simply to rearrange the fuel assemblies in each region such that Eq. (42) is minimized along the input integral path for each l and k starting with $l = k = 1$:

$$J = \min \left| \sum_k \sum_l \left(k^*_{\infty l,k} - k^*_{\infty k} \right) \right| \quad . \qquad (42)$$

For each l and k, a search is carried out among all the fuel assemblies $l' > l$ in region k. The k deviation becomes smallest at $l = 1$ for each region and increases for larger l. If the integral path is chosen carefully from the core center toward the outermost assemblies, the rearranged allocation will produce an acceptable power distribution.

As discussed earlier, the minimization of Eq. (42) is accomplished by the estimated EOC k'_∞ value. The primary principle behind allocating fuel assemblies by the integral path method is to adjust k^-_∞ and k^+_∞ among the fuel assemblies, where k^-_∞ and k^+_∞ mean the negative and positive sign of $k'_{\infty l,k} - k^*_{\infty k}$. To provide a symmetrical array, a specific rule is employed, called the integral path rule (IPR). The IPR applies to each region, starting in the order 1, 2, 3, . . . , N_a, to provide data for MIKDM. To attain symmetry, the path shown on the left in Fig. 3 is chosen for each subgroup of four assemblies. The order of each subgroup is arranged in a circular form, shown on the right in Fig. 3. On the edge of each region, small modifications are necessary to accommodate the region coupling. Thus, MIKDM and IPR would yield a symmetrical k^-_∞ and k^+_∞ array if the burnup distribution is uniform, since the sign of k deviation would appear periodically. The merit of this method stems from the fact that a power distribution calculation is not necessary.

V.E. Phase 5

By using the guess allocation generated by MIKDM in phase 4 as an initial guess, a direct search (an extended version of Naft's method[12]) is performed to optimize the allocation of each assembly. Since the kind of fuel assemblies that should be in each region has already been determined by G_{j0} and all constraints with the exception of the local mismatch factor are satisfied, the scale of the direct search is greatly reduced. In other words, Naft's method can be applied to each region. Furthermore, generation of a table for all regions is unnecessary since all the fuel assemblies in the low power regions cannot produce power peaking. In addition, it is not necessary to attempt all possible combinations of assembly exchanges in the region where the table is to be made, because only an exchange of high power assemblies with low power assemblies would reduce power peaking. On this basis, the following rules are employed:

1. Only regions where their maximum power densities are ranked within the first N_{pord} are considered to be candidates for fuel shuffling. Fuel assemblies in other regions are fixed. This ordering is made every time after a new table is generated; thus, the region of the candidate will vary from time to time.

2. Fuel assemblies are numbered in each region of the candidate from maximum to minimum power. A table is generated only for assemblies ranked within the first N_{try_k} to find N_{try_k} best candidates for exchange. (A table of $N_{\text{try}_k} * N_{\text{try}_k}$ is made for region k of the candidate.)

3. After the table has been generated, the program follows the same method as Naft's method, except that the table is erased only in the region concerned.

The optimization scheme has three modes: (a) exploratory, (b) standard, and (c) exhaustive search. In the exploratory mode, each variable is exchanged with every other variable. For each exchange, the objective function is the maximum value in the two-dimensional array. A table is created of N_{try_k} best choices for the first N_{try_k}-ranked assemblies in the selected region k. Noted in these N_{pord} tables are the power peaking values, assembly number, and the number of the assembly with which the exchange is to be made.

When the exploratory mode is completed, the scheme enters the standard search mode. The N_{pord} tables of exchange are searched for the lowest objective function value. When this value is found, the exchange is made, and any other shuffling in the table which includes these assemblies is erased. If the objective function is an improvement over the last guess, a new basis is formed. To determine the next best move, a search is again made of the tables. The new

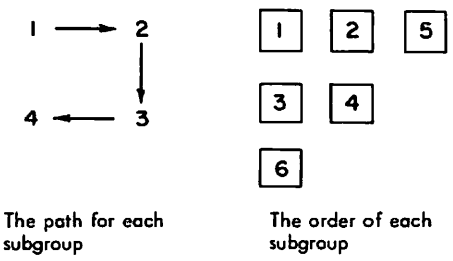

Fig. 3. Integral path rule—data path employed in MIKDM.

objective function is checked to determine if an improvement has been achieved. If so, all table entries containing the assemblies involved are eliminated, and a new basis is formed. If not, the next lowest value in these tables is searched for, and the process is repeated. The standard search continues until all entries in these tables have been utilized or until N_{fail} successive choices have ended in failure. When either occurs, the exploratory search mode is again called, and the entire process is repeated. The only successful exit from this scheme is the failure of a standard search move immediately following an exploratory search move.

If a standard search does not converge toward an optimum, the exhaustive search mode is called. In this case, only one base-point move is made after every exploratory search. A two-dimensional power distribution is calculated each time a trial is executed. In an effort to save computer time, two modes are prepared: a normal mode and a rapid mode. These differ in the allowed maximum number of source and void loop iterations. The normal mode is used as a base-point calculation, and the rapid mode is used in the table generation and trial calculation. In addition, fuel assemblies of the same type whose burnup differences are within ΔE_{band} are regarded as having the same nuclear properties. In this case, the power distribution calculation for the trial exchange of assemblies is skipped.

This optimization procedure is performed on the estimated EOC state as in phase 4. Since the estimate $k'_{\infty l,k}$ is calculated assuming the relation $P_{l,k} = P^{\dagger}_{k} \cdot f_{l,k}$, the calculated power is a rough approximation of a Haling power distribution. Since this is the most time-consuming part, it would be better to illustrate this method by a simple example of 25 grids which Naft and Sesonske[12] employed to optimize Eq. (43):

$$J = \min \left(\max X_{ij} \sum_{l=1}^{4} X^{l}_{ij} \right) \quad , \qquad (43)$$

where X_{ij} is the value of the independent variable at location (i,j) and X^{l}_{ij} is the value of the left, top, right, and bottom lateral neighbors. The value of X^{l}_{ij} on boundaries is regarded at 1.0.

First, the exact Naft method ($N_{reg} = 1$) is applied to obtain an optimal solution by using the same initial guess pattern as Naft employed. After 90 movements of the base point, the solution converged to J equal to 504. Next, the grid is artificially divided into two regions ($N_{reg} = 2$), and the optimal allocation is destroyed by rearranging assemblies within each region. No shuffling between regions is permitted. This allocation is used as an initial base point, which is shown in Fig. 4. The number of variables is 13 in region 1, and 12 in region 2.

Two calculations were performed under the following conditions:

Case 1: $N_{pord} = 1$; $N_{try\,1} = N_{try\,2} = 5$

Case 2: $N_{pord} = 1$; $N_{try\,1} = N_{try\,2} = 7$.

The number of exchanges in generating a table is ~50 for case 1 and ~63 for case 2. Computer running time for case 1 was 3.1 sec, and for case 2 was 9.9 sec, (CDC 6500). The optimized objective function was 672 and 468, and the number of base-point movements was 30 and 70, respectively. The exact Naft method for the same initial guess produced 528 over 70 movements of the base point with a computation time of 31.6 sec.

The optimal allocation in case 2 is shown in Fig. 5. One of the interesting results is that case 2 produces a better result than what had been thought to be optimal (504). Although the exact Naft method should cover the present approach, it was found that different search paths produced better results. The result presented here supports the method employed in phase 5.

	1	2	3	4	5
5	1.0 10.0	2.0 24.0	3.0 60.0	4.0 100.0	5.0 70.0
4	6.0 162.0	7.0 287.0	13.0 637.0	16.0 544.0	8.0 256.0
3	18.0 918.0	20.0 1460.0	23.0 1219.0	9.0 549.0	10.0 320.0
2	24.0 1416.0	25.0 1800.0	11.0 869.0	12.0 660.0	14.0 639.0
1	15.0 645.0	17.0 1020.0	19.0 950.0	21.0 1134.0	22.0 814.0

XX.X ← Independent Variable

YY.Y ← Power Distribution

NOTE: Maximum Power = 1800.0 at (2,2)

Fig. 4. Initial base-point allocation.

	1	2	3	4	5
5	13.0 468.0	18.0 414.0	7.0 441.0	20.0 420.0	12.0 444.0
4	16.0 352.0	2.0 166.0	24.0 312.0	1.0 78.0	15.0 360.0
3	6.0 390.0	25.0 375.0	3.0 270.0	19.0 361.0	10.0 460.0
2	23.0 460.0	4.0 364.0	22.0 440.0	5.0 330.0	11.0 363.0
1	9.0 414.0	21.0 462.0	8.0 464.0	14.0 434.0	17.0 459.0

XX.X ← Independent Variable

YY.Y ← Power Distribution

NOTE: Maximum Power = 468.0 at (1,5)

Fig. 5. Optimized allocation.

TABLE I

Specification of Reference BWR

Thermal output [MW(th)]	1300
Fuel assembly	
number of assemblies	400
active fuel length (m)	3.70
core lattice pitch (cm)	15.0
fuel enrichment (%)	
initial fuel	2.1
reload fuel	2.5
uranium in core (UO_2, ton)	85.0
MCHFR	1.9
Maximum linear heat generation rate (kW/ft)	17.5
Maximum burnup (GWd/T)	30.0
Maximum residence time (yr)	5.5
Average capacity factor	0.85
Core flow rate (lb/h)	4.3×10^7
Core inlet subcooling (Btu/lb)	-24.0

V.F. Phase 6

By using the optimized pattern of phase 5, a Haling power distribution and cycle length are accurately calculated. The resultant power distribution may be slightly different from the optimized result of phase 5 due to the approximation employed in estimating the EOC state in phase 5. The resulting cycle length may also differ slightly from that used in phases 1 through 5. Additional output from phase 6 includes moderator density, U_{ij}, burnup, E_{ij}, burnup-weighted void, V_{ij}, infinite multiplication factor, $k'_{\infty ij}$, fractional linear power density, $FLPD_{ij}$, critical heat flux ration, $CHFR_{ij}$, and core flow, F_{ij}. At the end of this calculation, a new fuel assembly file is generated, which is acceptable for the next cycle.

VI. RESULTS AND DISCUSSION

The application of the newly developed optimization procedure was successfully studied using a moderate-size BWR (see Table I for specifications). A complete ten-cycle study was conducted, starting with a uniform distribution of fresh fuel assemblies of 2.1% enrichment. Poison curtains were used in the first cycle to reduce the initial core reactivity and were withdrawn when the reactivity level was insufficient to maintain criticality. No attempt was made to optimize W_{j0} and G_{j0} for the first cycle. In other words, optimization was started at the beginning of the second cycle. The study itself, however, starts at the beginning-of-life of the reactor core with poison curtains in place.

Haling power-distribution and cycle-length calculations are made for the condition at which the reactor becomes just critical with all the control rods out and the poison curtain in place (step 1 of the first cycle). Next, the poison curtains are taken out of the core; another set of Haling power-distribution and accumulated cycle-length calculations are performed using the burnup and burnup-weighted void distribution at the end of step 1 as an initial condition (step 2 of the first cycle).

From the second cycle on, the cycle length was fixed at 1 yr, assuming a capacity factor of 0.85. Reload fuel assemblies are assumed to be of a single enrichment of 2.5%. Reinsertion of discharged fuel assemblies was considered only in the third cycle, because the discharged assemblies from the first cycle have a low amount of burnup.

A standard axial power distribution, which was obtained by averaging the power distribution from OPROD, a three-dimensional control-rod programming code,[19] over the entire first cycle period, was employed over all cycles.

Calculations were performed on a quarter core by assuming 90-deg rotation symmetry. An actual residence time limit of 6.5 yr and an average burnup of 4.75 GWd/T per year apply under the assumed capacity factor of 0.85. In the following calculations, the local reactivity constraints [Eqs. (18), (40), and (41)] are not taken into account in order to emphasize the optimization effects. In addition, the global power peaking factor, P_{max}, in Eq. (39) is assumed to be 1.30.

The core configuration (core map) of the reference reactor is shown in Fig. 6. The core is divided into five regions such that there are nearly an equal number of fuel assemblies in each region. When a three-region model is employed, regions 1, 2 and 3, 4 become the first and second regions of the new model. The number in the core map indicates the integral path that is used to generate an initial guess allocation in phase 4. This path follows the IPR described in Sec. V. Fuel assemblies in region 5 are orificed to reduce the channel flow because of their low power densities.

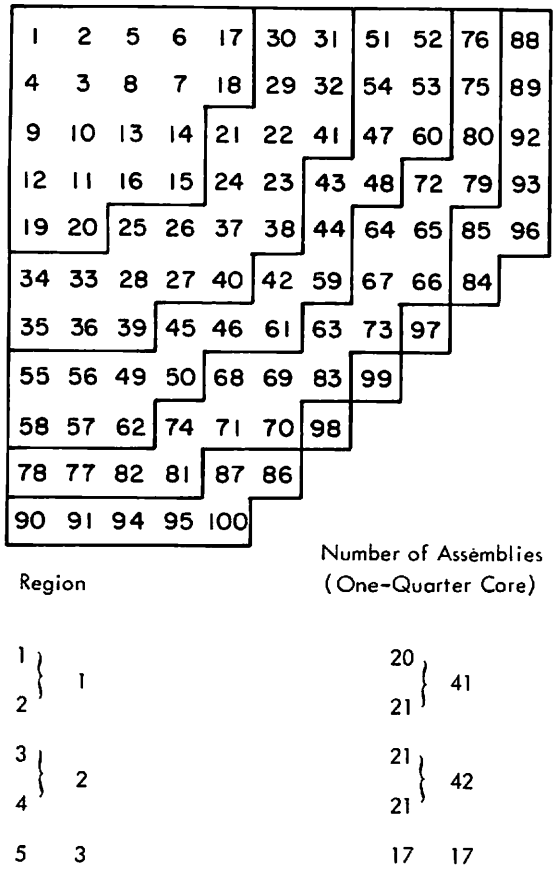

Fig. 6. Core configuration of reference BWR and integral path for MIKDM.

The results of the first cycle are summarized in Table II. By using the EOC state of the first cycle as an initial condition, an optimal refueling schedule was generated for ten cycles. Figure 7 indicates the number of fresh fuel assemblies loaded in each region and the total over the entire core with cycle. Although strong transients exist for the first four cycles, convergence to an equilibrium distribution is attained from approximately the fifth cycle on.

The results indicate that at the third cycle all the discharged assemblies from the first cycle are reinserted and burnt to nearly the end of their expected life. When the equilibrium cycle is reached, the number of fresh fuel assemblies required is ~72, which is 1 for every 5.56 assemblies in the total core. This corresponds to a mixed five and six batch-refueling scheme, which is contrary to the current four or mixed four and five batch-refueling practice used.

Figure 8 indicates the optimal EOC $k^*_{\infty k}$ distribution, which is one of the components of W'_{j0}. After a small transient at the second and third cycles, optimal W'_{j0} approaches an equilibrium distribution. The equilibrium distribution is characterized by a sharp depression in k_∞ in the

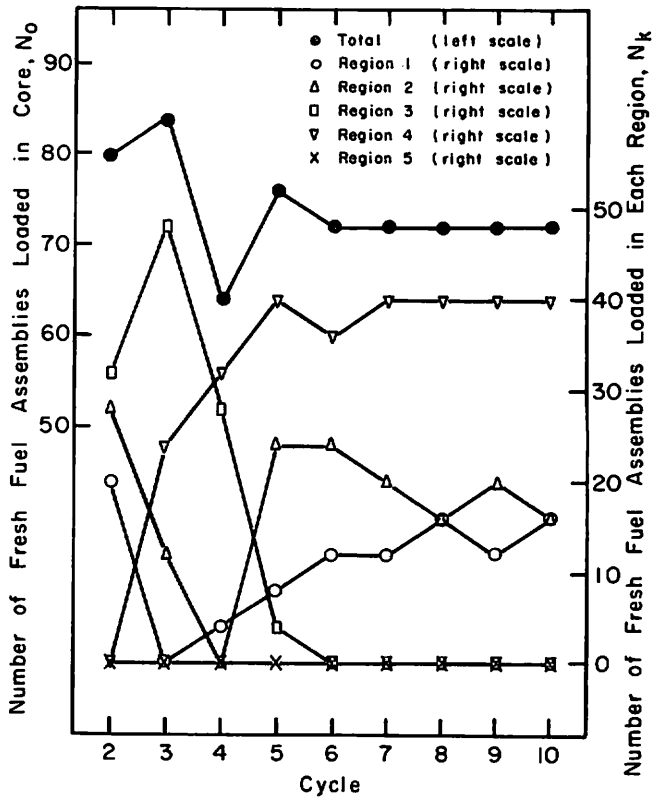

Fig. 7. Number of fresh fuel assemblies loaded by cycle for the optimal refueling schedule.

TABLE II

Characteristics of First-Cycle Refueling Schedule

Step 1 (poison curtain in)	
Core average burnup (GWd/T)	7.56
Length (yr)	1.59
Length (full power years)	1.35
Radial power peaking factor	1.29
MFLPD	0.799
MCHFR	3.295
Step 2 (poison curtain out)	
Core average burnup (GWd/T)	3.52
Length (yr)	0.74
Length (full power years)	0.63
Radial power peaking factor	1.20
MFLPD	0.743
MCHFR	3.697
Cycle length (yr)	2.33
Cycle length (full power years)	1.98

fifth region. This distribution is considered to be an optimal terminal state. It is reasonable that the optimal k_∞^* distributions in the transient cycles have higher values in region 5 than the equilibrium value, because few fuel assemblies in early cycles have attained sufficient burnup to produce a region of low k_∞ value.

It is interesting to note from Figs. 7 and 8 that no fresh fuel assemblies are loaded at an equilibrium cycle in region 3 where the target k_∞^* has the highest values, although in transient cycles the number loaded is very large. It is understandable that no fresh fuel assemblies are loaded at any cycle in region 5, because the target k_∞^* is of low value. In summary, about one-half of the fresh fuel assemblies are loaded in region 4, and the rest are properly scattered in regions 1 and 2 after an equilibrium cycle is attained. This means that approximately one-half of the assemblies in region 4 and one-fifth of the assemblies in regions 1 and 2, respectively, are fresh fuel assemblies.

Figure 9 indicates the burnup distribution of assemblies with cycle. Note that an equilibrium distribution is approached at approximately the sixth cycle. Although there are some abrupt changes in burnup among assemblies of different batches, the burnup distribution is generally uniform rather than stepwise.

The burnup distribution of assemblies in each region with cycle is shown in Fig. 10. An equilibrium distribution of burnup is indicated at approximately the sixth cycle; however, this distribution is not uniform in each region, except region 5. Note the variation of the distribution among the different regions. The burnup distribution has a tendency to split into groups toward the fourth region, starting from the first region.

The fact that this burnup distribution approaches an equilibrium distribution means that the fuel shuffling scheme also approaches an equilibrium scheme. As can be seen from Figs. 8 and 10, the target distribution W'_{j0} converges more rapidly to an equilibrium distribution than does the shuffling scheme G_{j0}.

Figure 11 describes the burnup of the discharged fuel assemblies with cycle. The average burnup approaches an equilibrium value of ~26 GWd/T from the seventh cycle onward. Although two types of fuel with different enrichments (in-

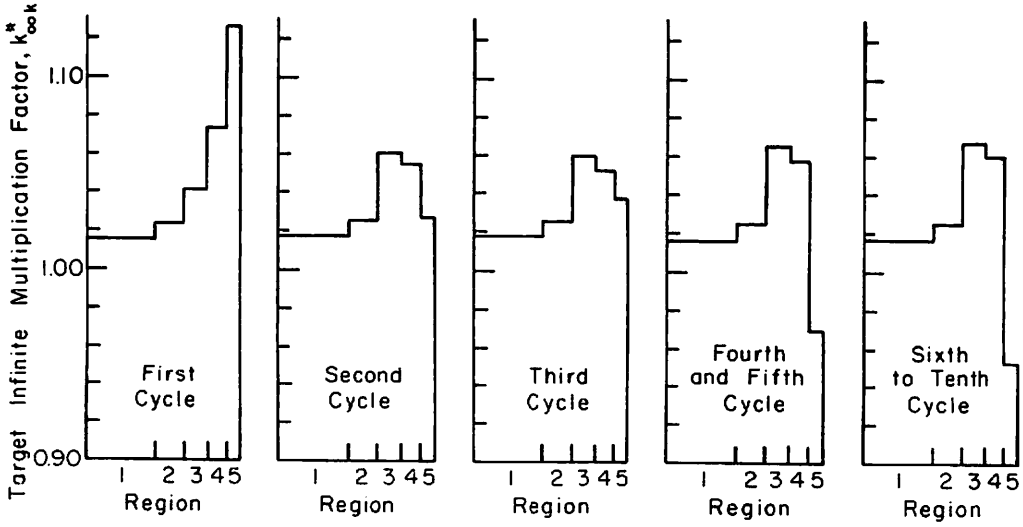

Fig. 8. Optimal target $k^*_{\infty k}$ distribution by cycle for the optimal refueling schedule.

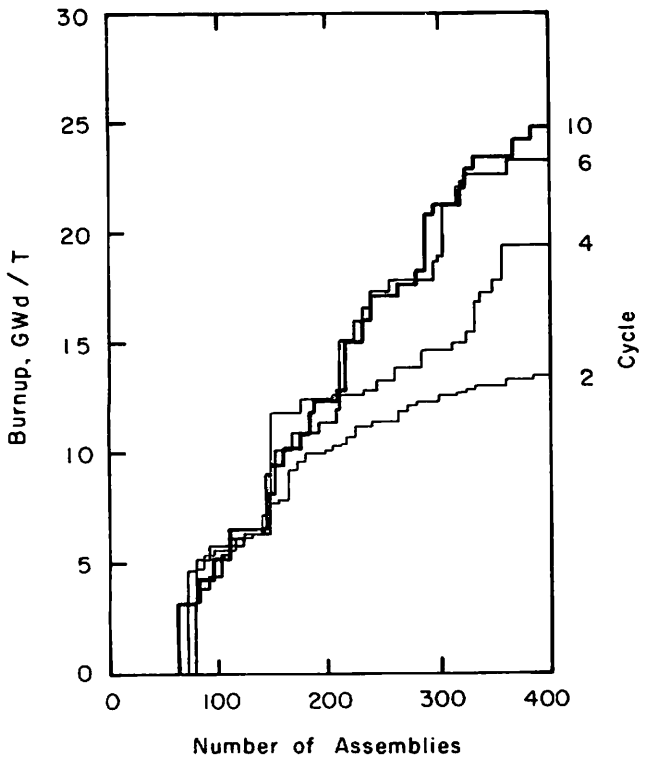

Fig. 9. Burnup distribution of assemblies in the core by cycle for the optimal refueling schedule.

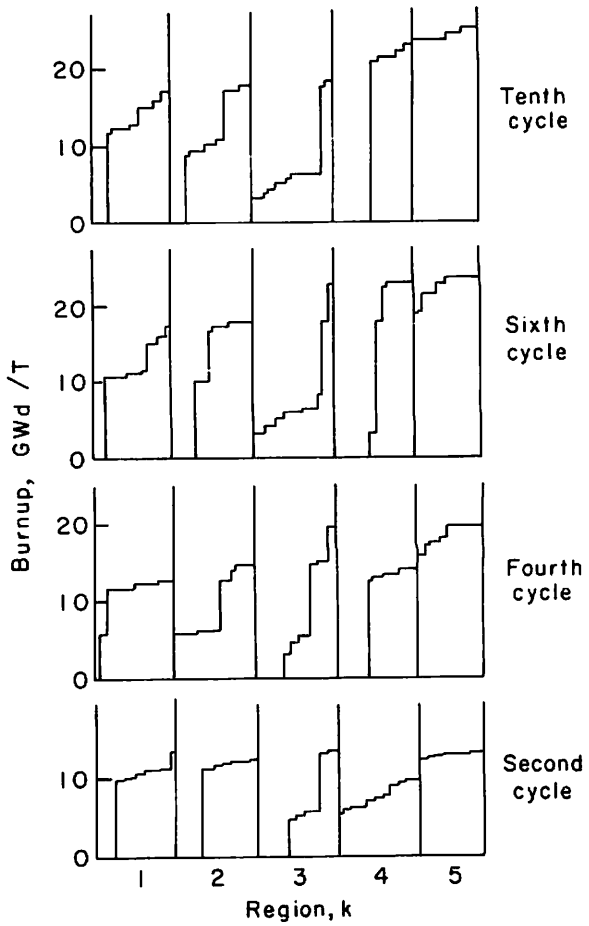

Fig. 10. Burnup distribution of assemblies in each region for the optimal refueling schedule.

itial fuel and reload fuel) are used, at each cycle a threshold burnup level exists which is indicated as the minimum burnup of the discharged fuel assemblies.

Figure 12 describes the change in the minimized radial power peaking factor [the minimized maximum fractional linear power density (MFLPD)] with cycle. There are three results. The first result (Δ) refers to the initial value of the assembly allocation generated by the minimum integral k-deviation method in phase 4. The second result (o) describes the minimized value of the assembly allocation by the direct search method in phase 5. The final result (•) is the recalculated value of the direct search by using the exact power burnup iteration in phase 6 (Haling calculation). The difference between "o" and "•" values is a measure of the error introduced by the approximation of the estimated EOC state. Power peaking values also indicate a tendency to approach an equilibrium value after the transient cycles have elapsed (after the sixth cycle). Although these power-peaking values are somewhat higher than are considered reasonable for current design, ample margin exists for MFLPD. These values are acceptable when considering that the power peaking factor of the target distribution, P_{max}, is set at

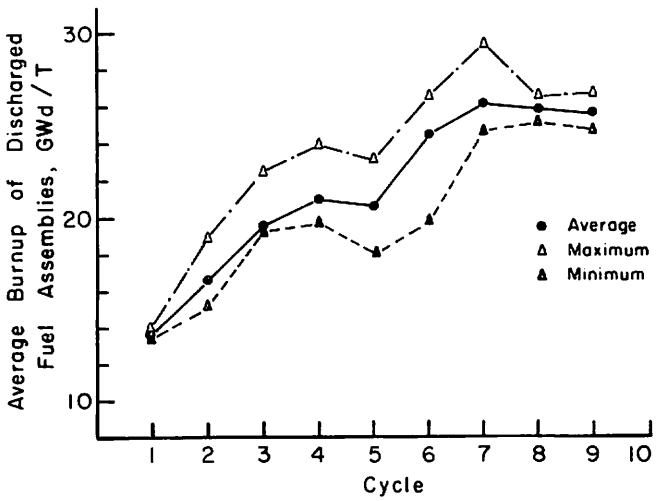

Fig. 11. Average burnup of discharged fuel assemblies with cycle for the optimal refueling schedule.

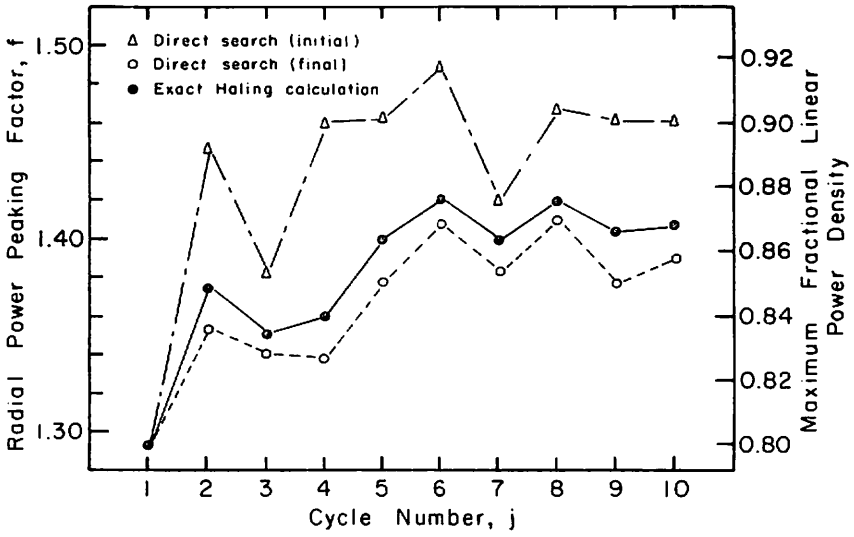

Fig. 12. Minimized radial power peaking factor and minimized maximum fractional linear power density with cycle for the optimal refueling schedule.

1.30, which is obtained by using the nuclear constants averaged over each region.

The power distribution of the first cycle is very flat compared with the distributions of later cycles. The reason for this is that no irregularities of k_{∞}^{BOC} exist among assemblies. Thus, a strong incentive exists to optimize the refueling schedule from the first cycle by using discharged assemblies from another reactor or by using more than one enrichment.

Figure 13 describes the change in the MCHFR with cycle. Although the accuracy of this result is questionable, because of critical heat flux ratio calculations which require accurate quality and power distribution in the axial direction as well as channel flows, ample margin exists in the MCHFR.

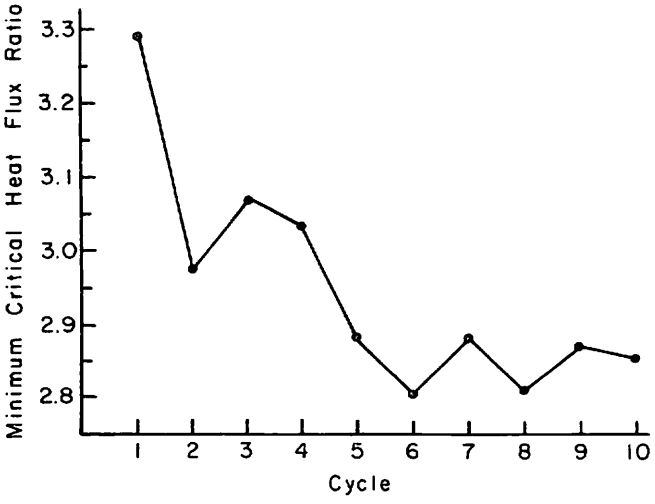

Fig. 13. Minimum critical heat flux ratio by cycle for the optimal refueling schedule.

Under the condition of Rt_{max} limit of 5.5 full power years and an E_{max} limit of 30 GWd/T, some assemblies are forced out of the core (discharged) at the sixth cycle. Although all these assemblies reach the residence time limit, their number is less than the required number of fresh fuel assemblies. No assemblies are forced out of the core due to the maximum burnup limit, although some are prohibited from being placed in regions of high power density (regions 1, 2, and 3).

The results of this study produced a spatially irregular k_{∞}^{EOC} distribution with certain patterns associated with the regionwise shuffling of assemblies. After the achievement of equilibrium, the data indicated that a shuffling rule may exist which could predict the regionwise location of an assembly cycle by cycle through its entire life. As a general rule, assemblies could be classified within three prediction groups with the shuffling patterns shown in Table III. As a typical example, consider prediction group 1 at an equilibrium cycle. The assembly begins and spends its first

TABLE III

Shuffling Rules at Equilibrium

Region Number (Cycle to Cycle)	
Group 1	1 → 3 → 1 → 2 → 5 (5) or 1 → 3 → 1 → 3 → 5 (5)
Group 2	2 → 3 → 1 → 2 → 5 (5) or 2 → 3 → 1 → 3 → 5 (5)
Group 3	4 → 3 → 2 → 1 → 4 (5) or 4 → 3 → 2 → 2 → 4 (5)

cycle of life in region 1, moves to region 3 for the second cycle, moves back to region 1 after another cycle, then to region 2, and finally completes its life in region 5. In every group case, the final discharge point (i.e., region) occurs from region 4 or 5.

To illustrate how each phase works in greater detail, the results of the eighth cycle, which is thought to be representative of an equilibrium cycle, are shown as an example. Figure 14 indicates the process of optimization of W'_{j0} in phase 1. The burnup E_3 of region 3 converges to 21.5 GWd/T at the seventh iteration. Linear programming gives an inaccurate result near the boundary of E_3, beyond which there is no feasible solution. The corresponding optimal EOC state W'_{j0} is shown in Fig. 15 by dotted lines. The extended result is shown by solid lines (phase 2). Note that $P_{max} = 1.30$.

The integerized optimal solution is shown in Table IV (phase 3). A level width, ΔB, of 0.7 GWd/T generates 26 burnup levels. The average estimated EOC $k_{\infty k}$ differs slightly from the target because of integerization effects, but the average local mismatch factor is still very close to unity (see Table V).

In phase 4, a guess allocation is calculated by employing the minimum integrated k-deviation method. The output of phase 4 is used as input to phase 5 where a final optimal allocation of assemblies is made. Figure 16 indicates how the assembly allocation is applied in reducing the power peaking factor. The solid large dot (●) indicates the initial base point at each table generation. The solid small dot (•) indicates a successful movement of the base point. The cross (×) indicates unsuccessful trials. Due to the inaccuracy of the rapid mode calculation, the power

TABLE IV

Integerized Optimal Solution of the Regionwise Shuffling Scheme for the Eighth Cycle (Phase 3)

Level	Number of Assemblies by Region					Total Number of Assemblies	Original Number of Assemblies in File
	Region 1	Region 2	Region 3	Region 4	Region 5		
1	4	4	0	10	0	18	0
2	0	0	3	0	0	3	3
3	0	0	1	1	0	2	2
4	0	0	2	0	0	2	2
5	0	0	3	0	0	3	3
6	0	0	8	0	0	8	8
7	0	5	0	0	0	5	5
8	0	2	0	0	0	2	2
9	0	2	0	0	0	2	2
10	2	0	0	0	0	2	2
11	7	0	0	0	0	7	7
12	1	0	0	0	0	1	1
13	1	0	0	0	0	1	1
14	3	0	0	0	0	3	3
15	2	0	0	0	0	2	2
16	0	2	0	0	0	2	2
17	0	4	0	0	0	4	4
18	0	2	2	0	0	4	4
19	0	0	2	0	0	2	2
20	0	0	0	1	0	1	1
21	0	0	0	4	0	4	4
22	0	0	0	5	0	5	5
23	0	0	0	0	6	6	6
24	0	0	0	0	7	7	7
25	0	0	0	0	4	4	9
26	0	0	0	0	0	0	5
Total	20	21	21	21	17		
k'^{a}_{∞}	1.0262	1.0237	1.0614	1.0642	0.9486		
$\bar{f}^{+b}_{k}$	1.0030	0.9971	0.9961	0.9965	0.9977		

[a] Average estimated EOC k_{∞}.
[b] Average local mismatch factor.

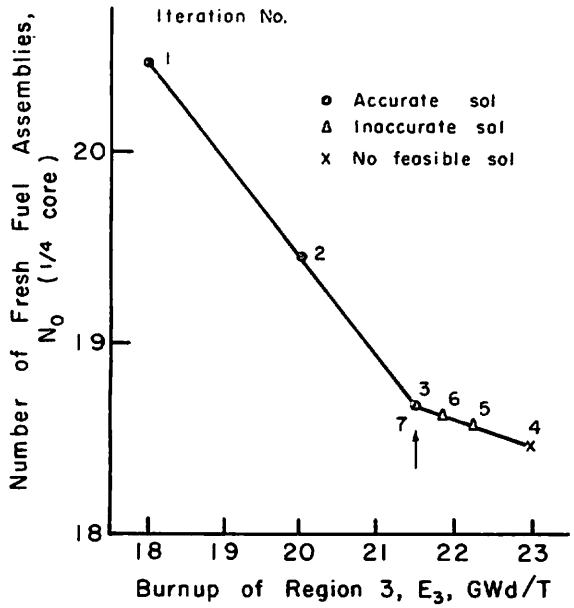

Fig. 14. Process of optimization of W'_{j0} at phase 1 of the eighth cycle for the optimal refueling schedule.

peaking factor increases at times. After 104 trials, of which 52 were successful, the optimal allocation was obtained with a power peaking factor reduction from 1.466 to 1.410. Calculational conditions are also given in Fig. 16. The final power distribution (phase 6) is calculated by the exact power-burnup iteration method (Haling principle). These results are given in Table V. The cycle length calculated in phase 6 is 0.993 yr, only slightly smaller than the expected value of 1.0.

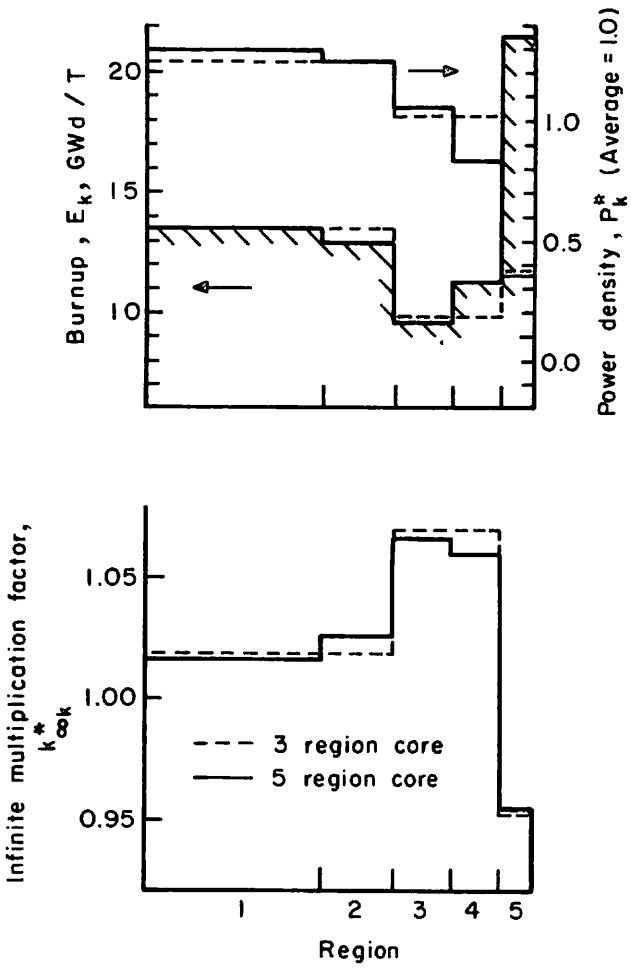

Fig. 15. Optimal EOC state extended to a five-region core for the eighth cycle (phase 2).

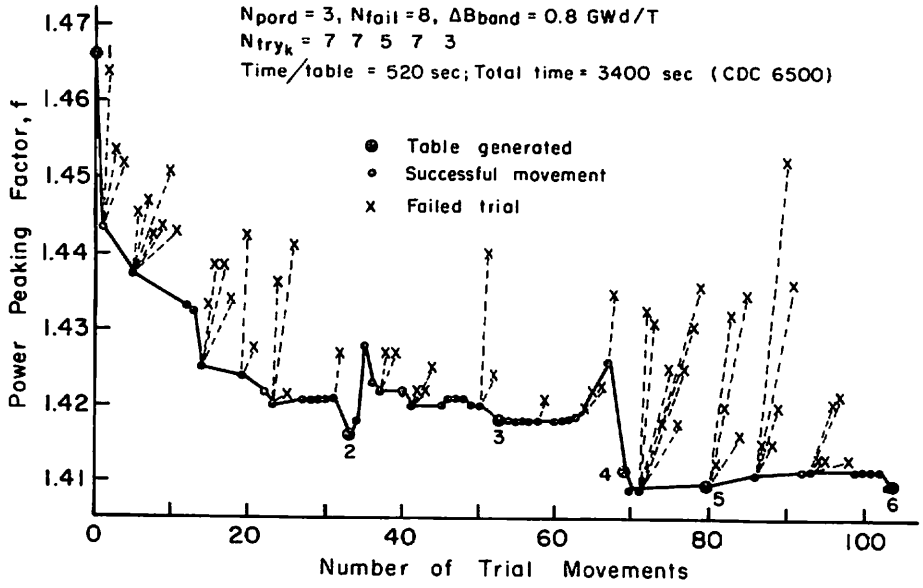

Fig. 16. Direct search calculations to an optimal allocation for the eighth cycle (phase 5).

TABLE V

Comparative Region-Averaged Data for Target W'_{j0} for Optimized Allocation (Eighth Cycle)

Region	1	2	3	4	5
P^*_k	1.290	1.249	1.158	0.836	0.359
P_k	1.264	1.256	1.168	0.842	0.361
l'^*_k	0.571	0.581	0.605	0.683	0.761
l'_k	0.577	0.579	0.604	0.681	0.759
$k^*_{\infty k}$	1.017	1.026	1.067	1.059	0.953
$k_{\infty k}$	1.024	1.024	1.064	1.058	0.951

The computing time per cycle is ~1 hr, using a CDC 6500 computer; 95% of this time is consumed in phase 5, the direct search method.

Thus far, only the optimal refueling schedule has been discussed. To best evaluate its merits quantitatively, a comparative study was also conducted which is referred to as the partially optimized refueling schedule. In this case, optimization of only G_{j0} is considered. The target W_{j0} is fixed at the values of the first cycle, which corresponds to the fuel loading scheme that makes k^{BOC}_{∞} uniform in a region-averaged manner.

Figure 17 shows the number of fresh fuel assemblies loaded in each region and the total over the whole core with cycle. In contrast with the optimal refueling schedule, the number of assemblies in each region does not converge to an equilibrium value. However, its total approaches an equilibrium value of 76, with much greater fluctuations than for the optimal refueling schedule.

Figure 18 indicates the burnup distribution of assemblies in each region with cycle. This distribution begins to approach an equilibrium distribution at approximately the sixth cycle; however, its fluctuations with cycle are much greater than those of the optimal refueling schedule. It is interesting to compare these distributions with those of the optimal refueling schedule. The burnup distributions of regions 1 and 2 are similar in each method. The burnup distribution of region 5 of the partially optimized schedule is similar to that of region 3 of the optimal schedule, and the burnup distribution of region 3 of the partially optimized schedule is similar to that of region 4 of the optimal refueling schedule. It is evident that this distribution is strongly related to the k^*_{∞} value. From the above results, it is clear that the optimal refueling schedule has more stable characteristics than does the partially optimized schedule.

The difference in the fresh fuel requirements is shown in Fig. 19 in terms of the accumulated

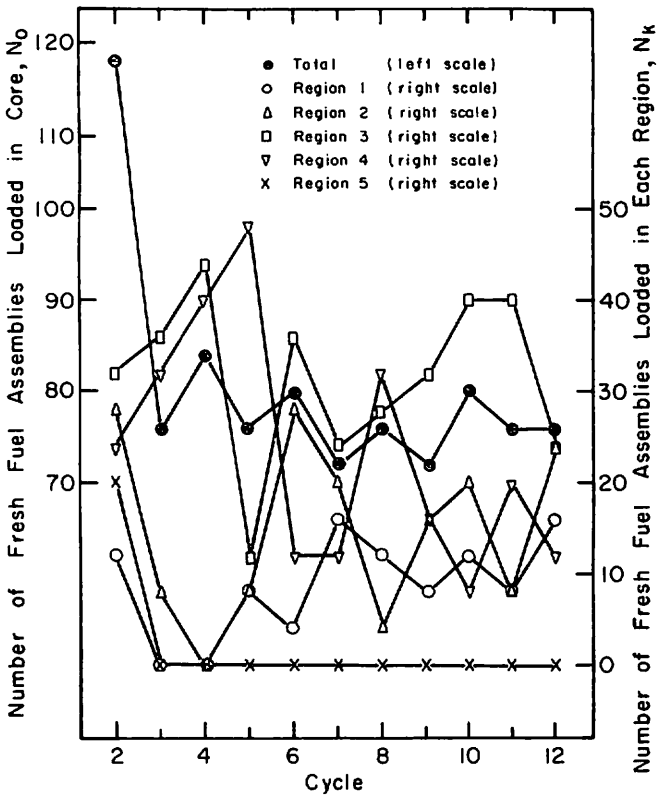

Fig. 17. Number of fresh fuel assemblies loaded by cycle for the partially optimized refueling schedule.

number of fresh fuel assemblies with cycle. The total number of fresh fuel assemblies required over ten cycles for the optimal case is 266 for a quarter core, or 1064 for an entire core. While in the case of the partially optimized refueling schedule a quarter core required 283 assemblies, or 1132 for an entire core. The difference between the two cases is therefore ~6.5%. Thus, the effect of optimizing W'_{j0} shows merit. Comparison with a mixed four and five (4.5) batch refueling schedule indicates savings of as much as 14%.

The difference in the fresh fuel requirement between the optimal and the partially optimized schedule is mostly in the first few cycles; this difference reflects strongly the effect of W'_{j0}. After an equilibrium cycle is achieved, the minimum number of fresh fuel assemblies necessary to recover the reactivity available, so that the reactor will operate for another cycle, depends still on W'_{j0} even if the solution is optimized G_{j0}.

VII. CONCLUSIONS AND RECOMMENDATIONS

A complete optimal reactor refueling schedule over a ten-cycle reactor period has been studied

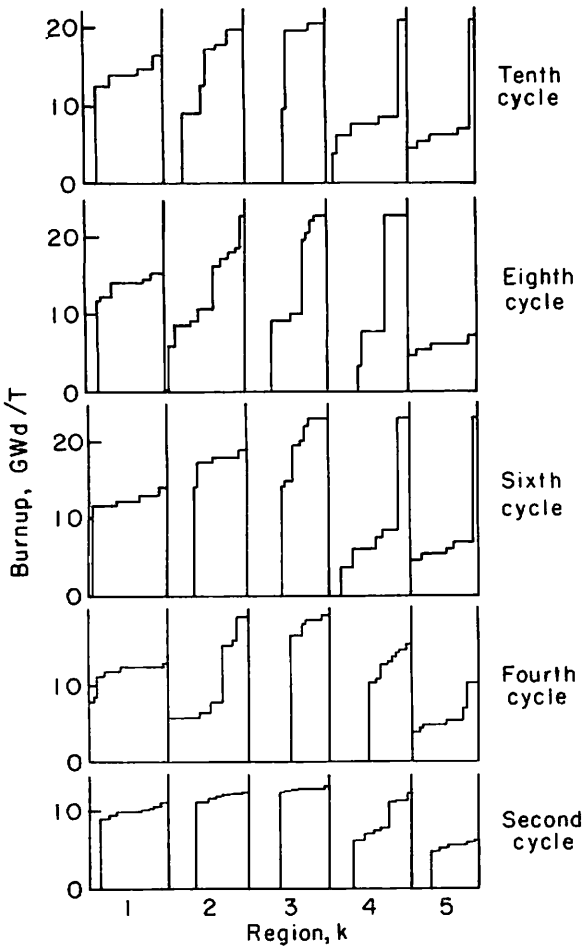

Fig. 18. Burnup distribution of assemblies in each region for the partially optimized refueling schedule.

by using a stagewise optimization method to simplify the handling of large numbers of decisions with emphasis given to the nuclear model. In the nuclear model, a two-dimensional nuclear-thermal-hydraulic-coupled code was used to calculate and optimize power distribution.

By assuming fixed initial and reload fuel enrichment, this method was applied to a typical medium-size BWR of 1300 MW(th) having 400 assemblies. Reinsertion of discharged fuel assemblies was permitted for the third cycle only. The results indicate a savings of ~14% (146 new fuel assemblies over ten cycles) of the fuel consumption in comparison with the conventional mixed four and five batch scatter-loading procedures. Compared with a partially optimized refueling schedule, a savings of ~6.5% is obtained.

The optimal refueling scheme does exhibit regularities in regionwise fresh fuel assembly reload and in the discharge of assemblies by region in cycle. Although the optimal BOC is no

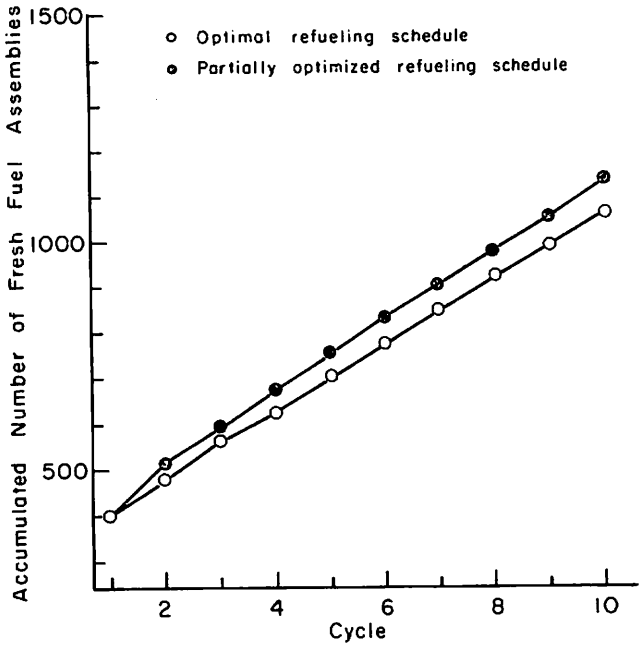

Fig. 19. Accumulated number of fresh fuel assemblies.

longer uniform, the resulting loading scheme gives a simple shuffling rule after the equilibrium cycle has been established.

The average computing time for one cycle of this study was ~1 h on a CDC 6500 computer, most of which was consumed by the direct search method (phase 5).

The optimization procedure appears applicable for actual practice, particularly considering the number of variables and constraints applied.

The following additional considerations are recommended for a future extension of this study:

1. inclusion of statistical decision theory to cope with unexpected outages and fluctuation of the capacity factor
2. investigation of other optimization functionals
3. optimization of the first cycle
4. more accurate treatment of the stuck-rod margin constraint.

Work is continuing on the development of generalized cycle-to-cycle shuffling patterns that evolve from this study for a variety of operational situations. These include the transient cycles as well as those after equilibrium has been achieved

ACKNOWLEDGMENTS

The authors would like to express their great thanks to K. O. Ott, P. J. Fulford, and O. H. Gailar for their fruitful discussions and encouragement.

This work was performed under the financial support of Hitachi, Ltd. and the Department of Nuclear Engineering while the first author stayed at Purdue University as a visiting scholar from Sept. 1972 to Aug. 1973.

REFERENCES

1. H. A. BRAMMER and G. R. PARKOS, "Refueling Methods for Large Boiling Water Reactors," *Proc. ANS Top. Mtg. Nuclear Performance of Power Reactor Cores*, TID-7672, U.S. Atomic Energy Commission (1964).

2. I. WALL and H. FENECH, "The Application of Dynamic Programming to Fuel Management Optimization," *Nucl. Sci. Eng.*, **22**, 285 (1965).

3. R. L. STOVER and A. SESONSKE, "Optimization of BWR Fuel Management Using An Accelerated Exhaustive Search Algorithm," *J. Nucl. Energy*, **26**, 673 (1969).

4. H. MOTODA, "Burnup Optimization of Continuous Scatter Refueling," *Nucl. Sci. Eng.*, **41**, 1 (1970).

5. H. MOTODA, "Optimal Control Rod Programming of Light Water Reactors in Equilibrium Fuel Cycle," *Nucl. Sci. Eng.*, **46**, 88 (1971).

6. J. R. FAGAN and A. SESONSKE, "Optimal Fuel Replacement in Reactivity Limited Systems," *J. Nucl. Energy*, **23**, 683 (1969).

7. T. HOSHINO, "In-Core Fuel Management Optimization by Heuristic Learning Technique," *Nucl. Sci. Eng.*, **49**, 59 (1972).

8. M. MÉLICE, "Pressurized Water Reactor Optimal Core Management and Reactivity Profiles," *Nucl. Sci. Eng.*, **37**, 451 (1969).

9. K. L. THOMSEN, "Self-Management, an Approach to Optimum Core Management of Thermal Reactors by Means of Ideal Burnup Distribution," Report No. 232, Danish Atomic Energy Commission Research Establishment Risö (1971).

10. T. O. SAUAR, "Application of Linear Programming to In-Core Fuel Management Optimization in Light Water Reactors," *Nucl. Sci. Eng.*, **46**, 274 (1971).

11. A. SUZUKI and R. KIYOSE, "Application of Linear Programming to Refueling Optimization for Light Water Moderated Reactor," *Nucl. Sci. Eng.*, **46**, 112 (1971).

12. B. N. NAFT and A. SESONSKE, "Pressurized Water Reactor Optimal Fuel Management," *Nucl. Technol.*, **14**, 123 (1971).

13. H. R. HOWLAND, C. N. DORNY, and R. L. STOVER, "Power Flattening and Loading Pattern Searches for Pressurized Water Reactors," *Trans. Am. Nucl. Soc.*, **16**, 170 (1973).

14. K. CHITAKARA and J. WEISMAN, "Optimal In-Core Fuel Management for Pressurized Water Reactors," *Trans. Am. Nucl. Soc.*, **15**, 655 (1972).

15. D. L. DELP, D. L. FISHER, J. M. HARRIMAN, and M. J. STEDWELL, "FLARE—A Three Dimensional Boiling Water Reactor Simulator," GEAP-4598, General Electric Co. (1964).

16. H. MOTODA, "Optimization of Control Rod Programming and Loading Pattern in Multiregion Nuclear Reactor by the Method of Approximation Programming," *Nucl. Sci. Eng.*, **49**, 515 (1972).

17. R. K. HALING, "Operating Strategy for Maintaining an Optimum Power Distribution Throughout Life," *Proc. ANS Top. Mtg. Nuclear Performance of Power Reactor Cores*, TID-7672, U.S. Atomic Energy Commission (1964).

18. A. ARIEMMA, G. L. PAROLA, M. P. GUALANDI, P. PERONI, and B. ZAFFIRO, "Accuracy of Power Distribution Calculation Methods for Uranium and Plutonium Lattice," *Nucl. Appl. Technol.*, **8**, 328 (1970).

19. H. MOTODA, T. KIGUCHI, and T. KAWAI, "Computer Program for Control Rod Programming of BWR," *Trans. Am. Nucl. Soc.*, **16**, 171 (1973).

20. P. GOLDSCHMIDT, "Minimum Critical Mass in Intermediate Reactors Subject to Constraints on Power Density and Fuel Enrichment," *Nucl. Sci. Eng.*, **49**, 263 (1972).